

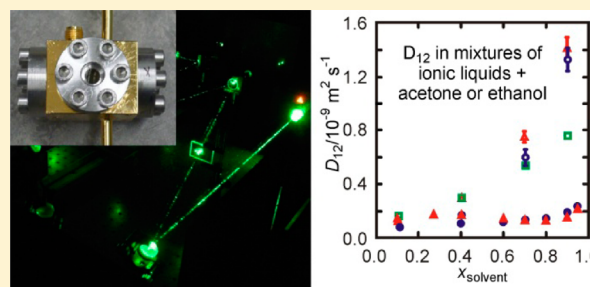
# Binary Diffusion Coefficients for Mixtures of Ionic Liquids [EMIM][N(CN)<sub>2</sub>], [EMIM][NTf<sub>2</sub>], and [HMIM][NTf<sub>2</sub>] with Acetone and Ethanol by Dynamic Light Scattering (DLS)

Michael H. Rausch,<sup>‡,†,\*</sup> Lisa Hopf,<sup>‡,§</sup> Andreas Heller,<sup>‡,†</sup> Alfred Leipertz,<sup>‡,†</sup> and Andreas P. Fröba<sup>‡,†</sup>

<sup>‡</sup>Erlangen Graduate School in Advanced Optical Technologies (SAOT), University of Erlangen-Nuremberg, Paul-Gordan-Straße 6, D-91052 Erlangen, Germany

<sup>†</sup>Institute of Engineering Thermodynamics (LTT), University of Erlangen-Nuremberg, Am Weichselgarten 8, D-91058 Erlangen, Germany

**ABSTRACT:** Mutual diffusivities for binary mixtures of the ionic liquids (ILs) [EMIM][N(CN)<sub>2</sub>] (1-ethyl-3-methylimidazolium dicyanide), [EMIM][NTf<sub>2</sub>] (1-ethyl-3-methylimidazolium bis(trifluoromethylsulfonyl)imide), and [HMIM][NTf<sub>2</sub>] (1-hexyl-3-methylimidazolium bis(trifluoromethylsulfonyl)imide) with acetone and ethanol were studied in dependence on composition in the temperature range from 283.15 to 323.15 K, applying dynamic light scattering (DLS). The influence of experimental parameters on the achievable uncertainties was analyzed to ensure the acquisition of accurate data in adequate measurement times. For all probed systems, increasing binary diffusion coefficients were found for increasing temperatures. The systematic variation of anion and cation of the investigated ILs as well as a comparison with the literature data demonstrates the considerable influence of different ions on the resulting binary diffusion coefficients. Mutual diffusivities were found to be lower for the mixtures with ethanol than for those with acetone, which could be related to the formation of hydrogen bonds between ethanol and the ions. Most of the investigated IL solvent mixtures show increasing binary diffusion coefficients with increasing solvent concentration. For the mixtures of [EMIM][NTf<sub>2</sub>] with ethanol, however, a minimum of the mutual diffusivities was found in the ethanol mole fraction range from 0.7 to 0.8, which may hint at the vicinity of a critical demixing point. The viscosity of the pure ILs turned out to be no reliable indicator for the mutual diffusivity in mixtures with the same solvent.



## 1. INTRODUCTION

Ionic liquids (ILs) are a new promising generation of working fluids for classical chemistry as well as for a wide range of industrial fields.<sup>1–5</sup> With more and more of the enormous number of possible anion–cation combinations resulting in ILs<sup>6</sup> being realized by adequate synthesis methods, reliable thermophysical property data are needed for the design of processes and apparatuses in which these liquids can be applied. As in technical applications ILs are frequently used in combination with other ILs or solvents, not only the thermophysical properties of pure ILs are of importance, but also those of corresponding mixtures.

An important property of such mixtures is the mutual diffusivity because it strongly affects, for example, separation processes<sup>7</sup> or catalytic reactions.<sup>8–10</sup> For a catalytic reaction using an IL as a reactant, catalyst, or reaction medium, the mutual diffusivity and the solubility of the mixture components are decisive parameters regarding the selectivity and kinetics of the reaction. Thus, knowledge of these parameters helps to preselect the potentially best-suited IL for a certain reaction.

In binary mixtures of ILs with molecular liquids, in principle, four chemical species are present, which are the undissociated IL, the dissociated ions of the IL, and the molecular liquid. Thus, diffusive transport can be described with four flux

equations. Because of electroneutrality in each volume of the system, the fluxes of the dissociated anions and cations are not independent. Furthermore, the flux of the undissociated IL is connected to the fluxes of the dissociated ions via the dissociation equilibrium. Consequently, there is only one independent flux so that the equilibration of concentration gradients can be described by a single mutual diffusion coefficient for the whole system.<sup>11</sup>

In the literature, hardly any mutual diffusion coefficients can be found for mixtures including ILs.<sup>12</sup> This is a result of the limitations of available measuring methods. Because of the high viscosity of most ILs, the Taylor dispersion technique can be applied only in the regime of infinite dilution.<sup>13–15</sup> For the digital image holography, the slow diffusion processes in ILs cause measuring times up to several days in the salt-rich region.<sup>16</sup> Other techniques based on the analysis of time-dependent absorption of gaseous solutes in ILs are restricted to low solute concentrations, where Henry's law is valid.<sup>17–20</sup> With binary mixtures consisting of the ILs [EMIM][EtSO<sub>4</sub>] (1-ethyl-3-methylimidazolium ethylsulfate) or [EMIM][MeSO<sub>3</sub>] (1-ethyl-

Received: June 21, 2012

Revised: January 23, 2013

Published: January 24, 2013



3-methylimidazolium methanesulfonate) and six different liquid molecular solvents, we recently demonstrated that dynamic light scattering (DLS) is a suitable technique for measuring mutual diffusivity data of such systems over the complete concentration range.<sup>21</sup>

In the present study, the influence of different cations and anions on the mutual diffusivity is studied for mixtures of systematically chosen ILs with acetone and ethanol at atmospheric pressure in the temperature range from 283.15 to 323.15 K. In detail, two ILs based on the [EMIM] cation, [EMIM][N(CN)<sub>2</sub>] (1-ethyl-3-methylimidazolium dicyanide) and [EMIM][NTf<sub>2</sub>] (1-ethyl-3-methylimidazolium bis(trifluoromethylsulfonyl)imide), as well as another IL based on the [NTf<sub>2</sub>] anion, [HMIM][NTf<sub>2</sub>] (1-hexyl-3-methylimidazolium bis(trifluoromethylsulfonyl)imide), were selected. For a reliable comparison of the obtained binary diffusion coefficients, the effects of boundary conditions such as measuring time and applied laser power on the accuracy of the results were systematically investigated in advance.

## 2. EXPERIMENTAL SECTION

**2.1. Materials and Sample Preparation.** [EMIM][NTf<sub>2</sub>] was synthesized by reacting equimolar amounts of [EMIM][EtSO<sub>4</sub>] and [Li][NTf<sub>2</sub>] (lithium bis(trifluoromethylsulfonyl)imide) in aqueous solution at about 333.15 K under vigorous stirring. The upper aqueous phase was decanted, and the lower phase containing [EMIM][NTf<sub>2</sub>] was separated, washed with distilled water, and dried at reduced pressure and elevated temperature. [EMIM][EtSO<sub>4</sub>] used for the synthesis was obtained by the procedure described by Maier et al.<sup>22</sup> The purity of [EMIM][NTf<sub>2</sub>] was proved by <sup>1</sup>H NMR analysis (JEOL, ECX-400 spectrometer, solvent dimethylsulfoxide-*d*<sub>6</sub>), where the total peak integral in the <sup>1</sup>H NMR spectrum was analyzed. [HMIM][NTf<sub>2</sub>] and [EMIM][N(CN)<sub>2</sub>] were purchased from Merck KGaA, Germany, and Lonza Group Ltd., Switzerland, respectively. Before use, the ILs were dried at about 333.15 K for a time period of ~5 h on a vacuum line (0.5 mbar) with an oil-sealed vacuum pump and a liquid nitrogen trap. For the dried ILs, the concentration of water was proved by Karl Fischer coulometric titration (Metrohm, 756 KF Coulometer) with an estimated expanded uncertainty (*k* = 2) of less than ±20%. The

**Table 1. Molecular Weight, Water Content by Mass, and Nominal Purity on a Molar Basis of the Studied ILs**

IL	<i>M</i> (g mol <sup>−1</sup> )	<i>w</i> (ppm)	purity (%)
[EMIM][N(CN) <sub>2</sub> ]	177.22	1855.1	>99
[EMIM][NTf <sub>2</sub> ]	391.34	23.5	>99
[HMIM][NTf <sub>2</sub> ]	447.42	225.6	>99

water contents, molar masses, and nominal purities of the used ILs are listed in Table 1. The solvents acetone and ethanol were purchased from Merck KGaA, Germany, with a nominal purity of >99.8%.

For the preparation of about 10–15 mL of each binary mixture, the pure components were drawn up into separate syringes. For the determination of the mixture composition, the syringes were weighed (Sartorius, BP 110 S, precision within ±1 × 10<sup>−4</sup> g) before and after filling the liquid into Schott flasks. For all substances, the absolute expanded uncertainty (*k* = 2) of the weighing procedure is estimated to be ±1 × 10<sup>−3</sup> g. This results in estimated absolute expanded uncertainties (*k* = 2) of the molar fraction of the molecular solvent *x*<sub>solvent</sub> ranging from ±1.6 × 10<sup>−5</sup> for the [EMIM][NTf<sub>2</sub>] ethanol

mixture with an ethanol mole fraction of *x*<sub>et</sub> = 0.95 to ±1.1 × 10<sup>−3</sup> for the [HMIM][NTf<sub>2</sub>] ethanol mixture with *x*<sub>et</sub> = 0.11. For all mixtures, the absolute uncertainty of the molar fraction decreases with increasing *x*<sub>solvent</sub>. Molar IL concentrations, *c*<sub>IL</sub>, in the mixtures were calculated assuming ideal volumetric mixing behavior. The complete mixture preparation was carried out under argon atmosphere. In addition, the filled Schott flasks were sealed to anticipate hydration of the ILs as well as solvent losses due to vaporization. Finally, the Schott flasks were shaken and stored for at least two days before the experiments to ensure good mixing. All sample-contacted parts and glassware used during the experiments were cleaned with water and ethanol, rinsed with deionized water, and dried.

**2.2. Mutual Diffusivities by DLS.** The DLS technique is based on the temporal analysis of the scattered light intensity reflecting the dynamics of microscopic fluctuations in pressure, temperature, and concentration. This noninvasive method gives access to different thermophysical properties in macroscopic thermodynamic equilibrium. The DLS method for the determination of mutual diffusivities is described in detail in the literature.<sup>21,23–26</sup> In the following, only the essential features relevant for the present study are summarized.

The DLS experiments for the measurement of mutual diffusivities are performed at heterodyne conditions where the scattered light from the sample is superimposed with a coherent reference beam. The heterodyne detection scheme was chosen because it allows an amplification of the small signal amplitudes observed for the concentration fluctuations. By choosing a scattering angle of Θ<sub>s</sub> = 90° in the present study, it could be ensured that the obtained intensity correlation functions are associated only with the equilibration of fluctuations in concentration.<sup>21</sup> For these conditions and if the signal is free of disturbances, the intensity correlation function, *g*<sup>(2)</sup>(τ), takes the form of an exponential,

$$g^{(2)}(\tau) = a + b \exp\left(-\frac{\tau}{\tau_c}\right) \quad (1)$$

In eq 1, *a* and *b* are experimental constants dependent not only on the intensities of the scattered and the reference light but also on effects due to the imperfect signal collection caused by the incoherent background and the finite detector area. The decay time, τ<sub>c</sub>, corresponds to the mean lifetime of the concentration fluctuations and is governed by the mutual diffusivity, *D*<sub>12</sub>, according to

$$\tau_c = \frac{1}{D_{12}q^2} \quad (2)$$

The decay time also depends on the modulus of the scattering vector, *q*,

$$q = \frac{4\pi n}{\lambda_0} \sin\left(\frac{\Theta_s}{2}\right) \quad (3)$$

which is given in terms of the fluid refractive index, *n*, the laser wavelength in vacuo, λ<sub>0</sub>, and the scattering angle, Θ<sub>s</sub>. The binary diffusion coefficient can be calculated from eq 2 with the decay time, τ<sub>c</sub>. The latter is obtained from least-squares fitting of eq 1 to the correlator data. The binary diffusion coefficients reported here are given with an expanded uncertainty (*k* = 2) calculated by error propagation in quadrature. In the figures, these uncertainties are represented by error bars. For their determination, the uncertainty of τ<sub>c</sub> is obtained from the standard deviation of the fit according

to eq 1 to the correlator data with a confidence interval of 95% ( $k = 2$ ). The uncertainty in  $q$  is determined on the basis of eq 3, where estimated expanded uncertainties ( $k = 2$ ) for  $\Theta_s$  of  $0.3^\circ$  and for  $n$  of 0.0005 are considered.

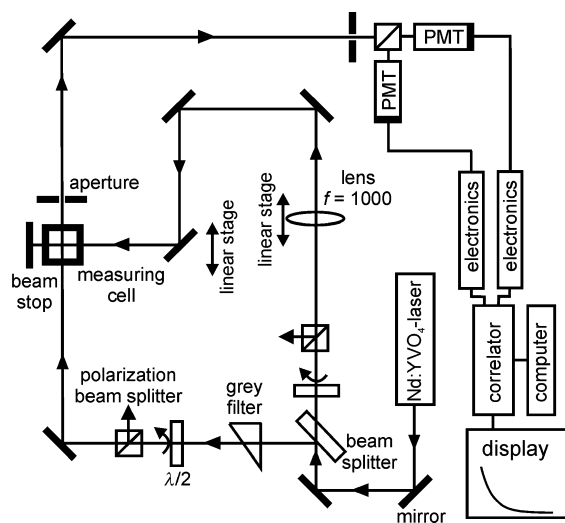


**Figure 1.** Optical and electronic arrangement of the applied DLS setup.

The optical and electronic arrangement of the applied DLS setup is schematically illustrated in Figure 1. From the coherent light of a frequency-doubled, continuous-wave Nd:YVO<sub>4</sub> laser with a wavelength of 532 nm, a reference beam is generated with a beam splitter. The overall laser power applied for the measurement of the mutual diffusion coefficients varies between 250 and 1500 mW, depending on the obtained light-scattering intensities. The main beam and the reference beam are adjusted regarding direction, focus, and intensity by the optical components shown in Figure 1. To obtain heterodyne conditions, the scattered light is superimposed with the reference beam in the observation direction. The latter is defined by two circular stops having a diameter of 0.5 mm each. One stop is installed behind the measuring cell, and the other one is placed in front of the photomultiplier tubes (PMTs). For the adjustment of  $\Theta_s = 90^\circ$ , the main beam as well as the reference beam are adjusted by backreflection from the glass windows of the measuring cell. After passing the stops, the scattered light superimposed with the reference beam is detected by two PMTs operating in cross-correlation mode to suppress afterpulsing effects. The DLS signals are amplified, discriminated, and fed to a digital single-tau correlator featuring 256 equally spaced channels. In the present study, the sample time per channel varied from 20 ns to 1.15  $\mu$ s, depending on the decay time of the concentration fluctuations.

The block-shaped sample cell made of stainless steel has four optical accesses. The volume of the cell is 4.8 mL. To avoid corrosion, the cell was coated with a thin layer of gold. For the experiments, the mixtures were added to the cell using a syringe under argon atmosphere, then the sample cell was closed. After investigation of each mixture, the sample cell was disassembled, cleaned with water and ethanol, rinsed with deionized water, and dried. The temperature control of the sample cell is realized by a water bath. The water temperature is adjusted by a laboratory thermostat (Julabo CF41) and measured with two calibrated Pt 100  $\Omega$  resistance probes with an absolute uncertainty of  $\pm 0.02$  K. One probe measures the temperature close to the sample cell while

the other probe is placed at the inlet of the water bath. At equilibrium conditions, the two temperatures did not differ by more than 46 mK. For the results given here, the temperature of the water bath measured close to the sample cell is assumed to correspond to the temperature of the sample. In this study, temperatures in the range between 283.15 and 323.15 K were adjusted in steps of 10 K, where the temperature stability was better than  $\pm 0.01$  K during an experimental run.

**2.3. Measurement of the Refractive Index.** The refractive indices of the mixtures at the laser wavelength  $\lambda_0 = 532$  nm applied in the DLS experiments are required for the determination of the moduli of the scattering vectors,  $q$  (eq 3). For the interpolation of the corresponding refractive indices, the refractive index,  $n_D$ , at the sodium line ( $\lambda_D = 589.3$  nm) as well as the refractive index difference,  $n_F - n_C$ , for the Fraunhofer lines ( $\lambda_F = 486.1$  nm and  $\lambda_C = 656.3$  nm) were measured with an Abbe refractometer (Leo Kuebler, R 6000 G). The sample temperatures studied in the DLS experiments were adjusted within  $\pm 0.1$  K using a laboratory thermostat and measured by a mercury thermometer with an absolute uncertainty of  $\pm 0.5$  K. The refractometer was calibrated with deionized water, and its expanded uncertainty ( $k = 2$ ) in the measurement of  $n_D$  and  $n_F - n_C$  is estimated to be less than  $\pm 0.0005$  and  $\pm 0.001$ .

### 3. RESULTS AND DISCUSSION

In the absence of disturbing signals as well as in the presence of only concentration fluctuations, the experimental correlation function,  $g^{(2)}(\tau)$ , can be represented by a single exponential, eq 1.<sup>21</sup> This holds for many cases within the present study, as exemplarily shown in Figure 2a.

For binary mixtures of [HMIM][NTf<sub>2</sub>] with acetone or ethanol, often a further signal in addition to the exponential mode originating from molecular diffusion was found at larger time scales (see, e.g., Figure 2b). Here, the signal reflecting the concentration fluctuations on a molecular level can be found within the first channels up to about 60  $\mu$ s and is superimposed with a long-term decay. Figure 2 depicts the dependence of this additional signal on concentration and temperature for two mixtures of [HMIM][NTf<sub>2</sub>] with ethanol mole fractions of  $x_{et} = 0.599$  and 0.950 at three different temperatures. For both concentrations, the long-term decay becomes more pronounced and is shifted to shorter times with increasing temperature. Furthermore, the observed behavior in the long-time range is more distinct for the lower ethanol concentration.

Regarding the origin of the additional signal, convective and optical effects have to be considered. Nevertheless, the observed dependence of this signal on temperature and concentration indicates that it could also originate from other, slower diffusion processes of particles, impurities, solvated ions, or even molecular agglomerations known as micelles. Because this behavior was found only for mixtures based on the IL [HMIM][NTf<sub>2</sub>], the long alkyl chain of its cation might be the reason for the formation of micelles or clusters. Micelle formation of ILs has been investigated in several studies<sup>27–30</sup> and tends to be more pronounced for ILs containing long alkyl chains in their anion or cation. However, for the determination of the decay time,  $\tau_C$ , from correlator data containing superimposed long-term signals such as those shown in Figure 2, these data can be fitted well with a quadratic term added to eq 1. Especially when both signals approach each other, the long-term signal influences the evaluation of the signal caused by molecular diffusion, which is reflected by larger uncertainties in  $\tau_C$ .

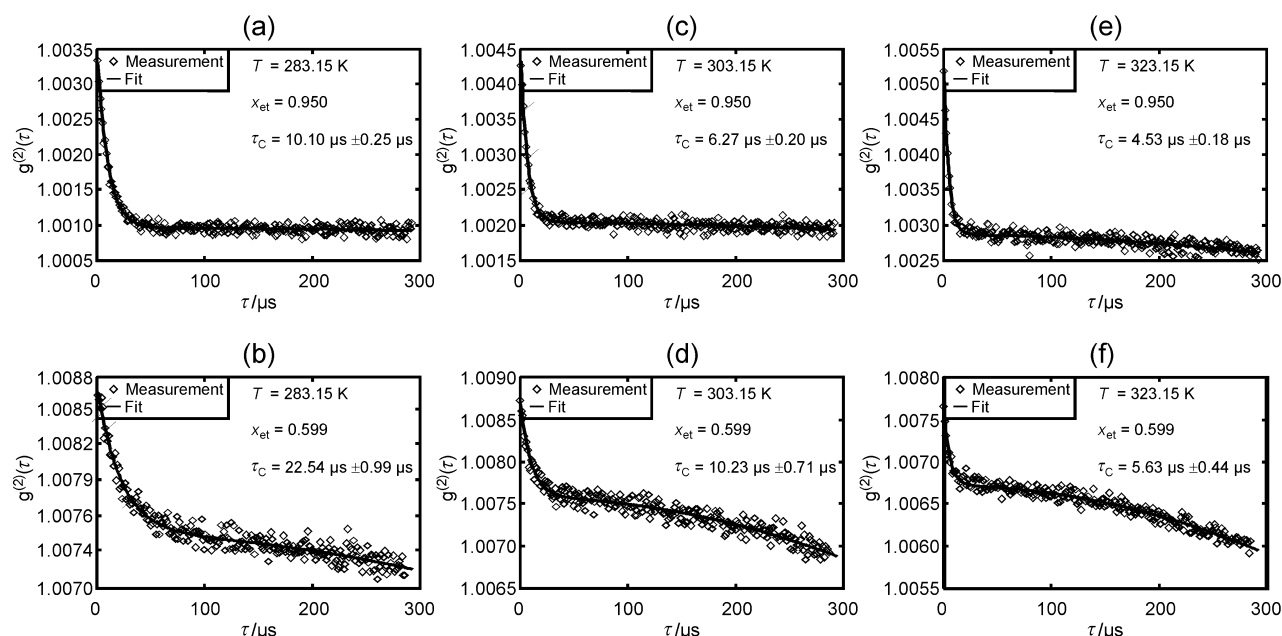


**Figure 2.** Correlation functions for mixtures of [HMIM][NTf<sub>2</sub>] and ethanol for varying temperatures and concentrations.

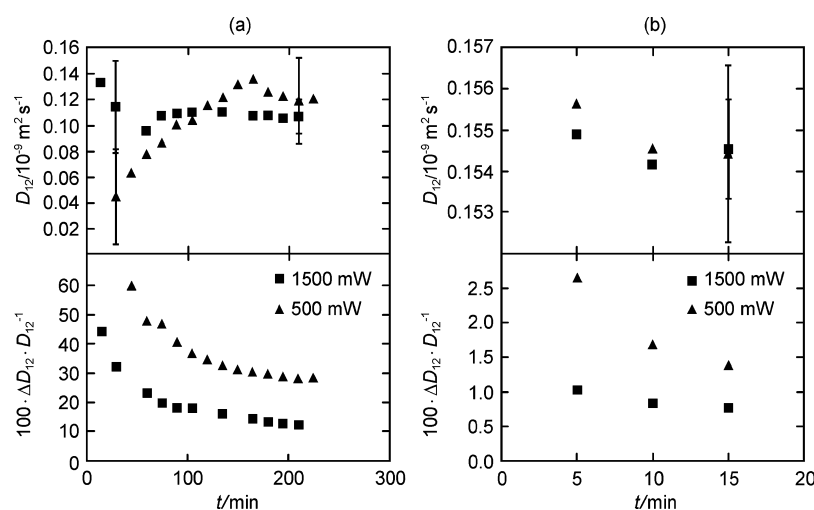


**Figure 3.** Binary diffusion coefficients and their relative uncertainties ( $k = 2$ ) as a function of measuring time and applied laser power at  $T = 283.15$  K for [EMIM][NTf<sub>2</sub>] ethanol mixtures with  $x_{\text{et}} =$  (a) 0.101 and (b) 0.950.

The first test measurements were intended to identify experimental requirements for obtaining mutual diffusivities with small uncertainties. The latter are influenced mainly by the light scattering intensities associated with concentration fluctuations. These intensities depend on boundary conditions such as the difference in the refractive indices of the pure mixture components, their concentration, and the applied laser power. In consequence, the resulting uncertainties in  $D_{12}$  for a given mixture are influenced by the measurement time as well as the applied laser power. Increased laser power allows shorter measurement periods, but may falsify the results, for example, by convective effects due to laser heating in the sample. In this context, two different mixtures of [EMIM][NTf<sub>2</sub>] with ethanol mole fractions of  $x_{\text{et}} = 0.1$  and 0.95 exhibiting very low and high light scattering intensities were investigated by applying laser powers of 500 mW and 1500 mW as well as different measuring times. For both mixtures, the binary diffusion coefficients and their expanded relative uncertainties ( $k = 2$ ) are shown as a function of measuring time and laser power in Figure 3.

In particular, the upper part of Figure 3a depicts that because of the statistics of the data acquisition, a certain measurement time is required until the exponential in the correlation function is developed to a degree that allows an accurate determination of  $\tau_C$  and, thus, of  $D_{12}$ . Within the combined uncertainties, however, the binary diffusion coefficients measured with different laser powers agree for all measurement times. This demonstrates that the resulting diffusion coefficients are independent of the applied laser powers. The same conclusions can be drawn for the mixture with  $x_{\text{et}} = 0.95$  (see the upper part of Figure 3b). Because the light scattering intensities for this mixture are distinctly larger, accurate  $D_{12}$  values are obtained within short measuring times. The expanded relative uncertainties in  $D_{12}$  shown in the lower part of Figure 3 indicate that these values tend to converge after  $\sim 200$  and 15 min for  $x_{\text{et}} = 0.1$  and 0.95. Because of larger light scattering intensities, the uncertainties are considerably smaller for the higher laser power after the same measuring time. As a result of the above findings, the experiments performed within this study were stopped as soon as the



**Table 2.** Refractive Index  $n_D$  at the Sodium Line ( $\lambda_D = 589.3$  nm), Refractive Index Difference  $n_F - n_C$  for the Fraunhofer Lines F ( $\lambda_F = 486.1$  nm) and C ( $\lambda_C = 656.3$  nm), Binary Diffusion Coefficient  $D_{12}$ , and Estimated Relative Expanded Uncertainty ( $k = 2$ ) in  $D_{12}$  for Binary Mixtures of [EMIM][NTf<sub>2</sub>] + Solvents

solvent	$x_{\text{solvent}}$	$T$ (K)	$n_D$	$n_F - n_C$	$D_{12}$ ( $10^{-9} \text{ m}^2 \text{ s}^{-1}$ )	$100 \times \frac{\Delta D_{12}}{D_{12}}$
ethanol	0.000	283.15	1.4273	0.0082		
	0.000	293.15	1.4254	0.0082		
	0.000	303.15	1.4228	0.0080		
	0.000	313.15	1.4200	0.0081		
	0.000	323.15	1.4171	0.0078		
	0.101	283.15	1.4262	0.0081	0.106	12.4
	0.101	293.15	1.4241	0.0081	0.138	13.5
	0.101	303.15	1.4215	0.0078	0.182	18.0
	0.101	313.15	1.4190	0.0079	0.235	18.3
	0.101	323.15	1.4167	0.0083	0.341	22.4
	0.271	283.15	1.4239	0.0081	0.113	4.8
	0.271	293.15	1.4208	0.0084	0.167	4.5
	0.271	303.15	1.4187	0.0081	0.244	6.8
	0.271	313.15	1.4168	0.0081	0.300	8.1
	0.271	323.15	1.4139	0.0074	0.387	7.7
	0.403	283.15	1.4212	0.0079	0.108	2.3
	0.403	293.15	1.4183	0.0082	0.163	2.5
	0.403	303.15	1.4159	0.0077	0.225	3.3
	0.403	313.15	1.4136	0.0075	0.294	3.7
	0.403	323.15	1.4110	0.0075	0.387	4.8
	0.600	283.15	1.4135	0.0077	0.093	1.4
	0.600	293.15	1.4107	0.0077	0.139	1.8
	0.600	303.15	1.4076	0.0074	0.202	2.2
	0.600	313.15	1.4048	0.0078	0.277	2.9
	0.600	323.15	1.4021	0.0079	0.379	3.1
	0.701	283.15	1.4083	0.0069	0.083	1.1
	0.701	293.15	1.4062	0.0083	0.126	1.3
	0.701	303.15	1.4040	0.0080	0.187	1.9
	0.701	313.15	1.4011	0.0076	0.257	2.2
	0.701	323.15	1.4001	0.0082	0.353	3.5
	0.800	283.15	1.4028	0.0076	0.082	0.8
	0.800	293.15	1.4000	0.0076	0.123	1.0
	0.800	303.15	1.3969	0.0077	0.181	1.2
	0.800	313.15	1.3942	0.0072	0.252	1.5
	0.800	323.15	1.3920	0.0073	0.343	1.7
	0.900	283.15	1.3888	0.0083	0.102	1.0
	0.900	293.15	1.3853	0.0076	0.146	1.1
	0.900	303.15	1.3834	0.0072	0.204	1.3
acetone	0.900	313.15	1.3801	0.0080		1.4
	0.900	323.15	1.3777	0.0101		1.8
	0.950	283.15	1.3797	0.0071		1.4
	0.950	293.15	1.3756	0.0077		1.7
	0.950	303.15	1.3724	0.0067		1.9
	0.950	313.15	1.3693	0.0068		2.1
	0.950	323.15	1.3658	0.0068		2.6
	1.000	283.15	1.3661	0.0064		
	1.000	293.15	1.3630	0.0065		
	1.000	303.15	1.3582	0.0070		
	1.000	313.15	1.3549	0.0065		
	1.000	323.15	1.3518	0.0072		
	0.103	283.15	1.4267	0.0082	0.096	9.7
	0.103	293.15	1.4236	0.0079	0.126	11.6
	0.103	303.15	1.4209	0.0081	0.201	10.1
	0.103	313.15	1.4186	0.0079	0.230	12.5
	0.103	323.15	1.4158	0.0079	0.308	12.9
	0.400	283.15	1.4202	0.0081	0.234	4.5
	0.400	293.15	1.4172	0.0079	0.297	5.6
	0.400	303.15	1.4147	0.0077	0.376	5.7
	0.400	313.15	1.4129	0.0079	0.484	4.7
	0.400	323.15	1.4098	0.0074	0.583	6.6
	0.699	283.15	1.4098	0.0077	0.621	4.7
	0.699	293.15	1.4051	0.0076	0.752	5.4
	0.699	303.15	1.4044	0.0078	0.846	6.9
	0.699	313.15	1.4038	0.0077	1.02	7.0
	0.699	323.15	1.4023	0.0078	1.17	8.0
	0.900	283.15	1.3873	0.0076	1.18	6.5
	0.900	293.15	1.3846	0.0077	1.42	5.6
	0.900	303.15	1.3807	0.0074	1.62	5.4
	0.900	313.15	1.3767	0.0075	1.85	9.7
	0.900	323.15	1.3728	0.0077	2.26	9.0
	1.000	283.15	1.3642	0.0070		
	1.000	293.15	1.3588	0.0069		
	1.000	303.15	1.3554	0.0069		
	1.000	313.15	1.3499	0.0071		
	1.000	323.15	1.3450	0.0073		

relative error no longer decreased significantly with time. Depending on the light scattering intensities obtained from the individual mixtures, the laser power was chosen for each measurement.

Two ILs based on the cation [EMIM] with the anions [N(CN)<sub>2</sub>] and [NTf<sub>2</sub>] as well as another IL having the anion [NTf<sub>2</sub>], [HMIM][NTf<sub>2</sub>], were tested in combination with the molecular solvents ethanol and acetone to study the influence of different ions on the mutual diffusivity. In most cases, four solvent mole fractions ( $x_{\text{solvent}} \approx 0.1, 0.4, 0.7, 0.9$ ) were investigated at temperatures varying in the range from 283.15 to 323.15 K in steps of 10 K. The measured refractive indices and mutual diffusivities are given in Tables 2–4. For  $D_{12}$ , the expanded relative uncertainties ( $k = 2$ ) are also given for each data point. For [EMIM][N(CN)<sub>2</sub>], only mixtures with acetone were investigated because shortly after mixing the IL with ethanol, particles precipitated for ethanol mole fractions of  $x_{\text{et}} = 0.7$  and  $x_{\text{et}} = 0.9$ . Because the light-scattering intensities due to particle diffusion are distinctly larger than those resulting from molecular diffusion, mutual diffusivities could not be measured for the [EMIM][N(CN)<sub>2</sub>] ethanol system.

For the comparison of all investigated systems, only the data obtained at  $T = 293.15$  K are exemplarily discussed. For the other temperatures, analog results were found. In Figure 4, the binary diffusion coefficients measured for the different systems are given as a function of the solvent mole fraction,  $x_{\text{solvent}}$ , as well as in dependence on the square root of the molar concentration of the IL,  $c_{\text{IL}}^{0.5}$ . The latter representation is commonly used in electrolyte work and serves for comparison of the present results with corresponding studies.

Except for the mixtures of [EMIM][NTf<sub>2</sub>] and [HMIM][NTf<sub>2</sub>] with acetone mole fractions of  $x_{\text{ac}} = 0.7$  and  $0.9$ , the error bars representing the expanded uncertainty of  $D_{12}$  are within the symbols. For all mixtures with acetone as well as for the mixtures of [HMIM][NTf<sub>2</sub>] with ethanol, the binary diffusion coefficient increases with increasing solvent concentration. This behavior is in agreement with decreasing viscosities of the mixtures, taking into account that the pure solvents ( $\eta_{\text{ac}} = 0.321$  mPa s at 293.15 K,<sup>31</sup>  $\eta_{\text{et}} = 1.187$  mPa s at 293.15 K<sup>32</sup>) show distinctly lower viscosities than the pure ILs ( $\eta = 22.8$  mPa s for [EMIM][N(CN)<sub>2</sub>] at 293.15 K,<sup>33</sup>  $\eta = 38.6$  mPa s for

**Table 3.** Refractive Index  $n_D$  at the Sodium Line ( $\lambda_D = 589.3$  nm), Refractive Index Difference  $n_F - n_C$  for the Fraunhofer Lines F ( $\lambda_F = 486.1$  nm) and C ( $\lambda_C = 656.3$  nm), Binary Diffusion Coefficient  $D_{12}$ , and Estimated Relative Expanded Uncertainty ( $k = 2$ ) in  $D_{12}$  for Binary Mixtures of [HMIM][NTf<sub>2</sub>] + Solvents

solvent	$x_{\text{solvent}}$	$T$ (K)	$n_D$	$n_F - n_C$	$(10^{-9} D_{12} \text{ m}^2 \text{ s}^{-1})$	$100 \times \frac{\Delta D_{12}}{D_{12}} \times$	solvent	$x_{\text{solvent}}$	$T$ (K)	$n_D$	$n_F - n_C$	$(10^{-9} D_{12} \text{ m}^2 \text{ s}^{-1})$	$100 \times \frac{\Delta D_{12}}{D_{12}} \times$
ethanol	0.000	283.15	1.4356	0.0080			acetone	0.800	313.15	1.3983	0.0069	0.268	2.7
	0.000	293.15	1.4329	0.0081				0.800	323.15	1.3958	0.0071	0.361	4.7
	0.000	303.15	1.4304	0.0079				0.900	283.15	1.3944	0.0071	0.135	1.5
	0.000	313.15	1.4276	0.0079				0.900	293.15	1.3912	0.0068	0.191	1.6
	0.000	323.15	1.4256	0.0079				0.900	303.15	1.3887	0.0067	0.254	1.9
	0.110	283.15	1.4339	0.0078	0.058	22.5		0.900	313.15	1.3857	0.0070	0.336	2.2
	0.110	293.15	1.4315	0.0081	0.080	22.5		0.900	323.15	1.3823	0.0069	0.418	2.6
	0.110	303.15	1.4288	0.0079	0.099	22.5		0.950	283.15	1.3824	0.0067	0.176	1.8
	0.110	313.15	1.4268	0.0079	0.121	20.5		0.950	293.15	1.3790	0.0066	0.236	1.8
	0.110	323.15	1.4242	0.0078	0.170	21.0		0.950	303.15	1.3759	0.0065	0.306	2.3
	0.396	283.15	1.4280	0.0081	0.076	5.2		0.950	313.15	1.3732	0.0065	0.394	2.4
	0.396	293.15	1.4264	0.0079	0.107	5.6		0.950	323.15	1.3693	0.0065	0.484	2.7
	0.396	303.15	1.4238	0.0078	0.146	6.0		0.401	283.15	1.4295	0.0080	0.130	8.3
	0.396	313.15	1.4210	0.0078	0.212	10.6		0.401	293.15	1.4258	0.0080	0.169	12.3
	0.396	323.15	1.4189	0.0076	0.308	7.7		0.401	303.15	1.4237	0.0078	0.193	8.9
	0.599	283.15	1.4214	0.0076	0.079	2.3		0.401	313.15	1.4208	0.0078	0.285	9.7
	0.599	293.15	1.4189	0.0076	0.120	3.0		0.401	323.15	1.4183	0.0077	0.361	10.3
	0.599	303.15	1.4163	0.0076	0.172	3.0		0.702	283.15	1.4160	0.0078	0.404	11.0
	0.599	313.15	1.4132	0.0076	0.239	3.5		0.702	293.15	1.4136	0.0077	0.600	9.9
	0.599	323.15	1.4113	0.0074	0.332	5.3		0.702	303.15	1.4108	0.0076	0.711	7.9
	0.703	283.15	1.4158	0.0077	0.088	1.6		0.702	313.15	1.4076	0.0079	0.895	5.7
	0.703	293.15	1.4138	0.0076	0.131	2.1		0.702	323.15	1.4050	0.0078	1.11	5.5
	0.703	303.15	1.4119	0.0072	0.184	2.5		0.901	283.15	1.3927	0.0076	1.04	9.7
	0.703	313.15	1.4084	0.0072	0.258	2.5		0.901	293.15	1.3889	0.0071	1.33	6.4
	0.703	323.15	1.4058	0.0075	0.336	3.1		0.901	303.15	1.3846	0.0074	1.47	6.1
	0.800	283.15	1.4068	0.0074	0.102	1.3		0.901	313.15	1.3809	0.0074	1.79	6.6
	0.800	293.15	1.4043	0.0070	0.146	1.7		0.901	323.15	1.3787	0.0074	1.91	5.2
	0.800	303.15	1.4016	0.0069	0.204	1.9							

[EMIM][NTf<sub>2</sub>] at 293.15 K,<sup>33</sup>  $\eta = 89.26$  mPa s for [HMIM]-[NTf<sub>2</sub>] at 293.15 K<sup>34</sup>). A correlation between mutual diffusivity and viscosity can often be observed because decreasing viscosity hints at increasing mobility of the molecules.<sup>16</sup> The measured mutual diffusivities are on the same order of magnitude as those reported in former studies.<sup>16,21</sup> For the ILs mixed with ethanol, the values are distinctly lower than those obtained for the mixtures with acetone, which corresponds to our previous results for mixtures with [EMIM][EtSO<sub>4</sub>].<sup>21</sup> This may be attributed to the formation of hydrogen bonds between ethanol and the ions, retarding the mutual diffusion process.

For the ILs [EMIM][NTf<sub>2</sub>] and [EMIM][N(CN)<sub>2</sub>] mixed with acetone, it is noticeable that the  $D_{12}$  values approximately match for  $x_{\text{ac}} = 0.1$  and  $0.4$ . With increasing acetone concentration, however, they increase more strongly for the mixtures based on [EMIM][NTf<sub>2</sub>], although the viscosity of pure [EMIM][NTf<sub>2</sub>] is higher than that of [EMIM][N(CN)<sub>2</sub>]. In this context, it has to be taken into account that both viscosity and mutual diffusivity depend on intermolecular interactions such as Coulomb or van der Waals forces. In addition, steric effects resulting from the geometries of the involved molecules and ions can be important. Comparing different systems, all of these influencing factors have to be considered, where different interactions may dominate the viscosity and diffusivity behaviors. The  $D_{12}$  results found for the acetone mixtures with the [EMIM]-based ILs show that the different forms of interaction seem to affect viscosity and diffusion differently. However, it should be mentioned that mixture viscosities allowing a more detailed evaluation of this behavior are not available. Compared

with our previous results for mixtures of [EMIM][EtSO<sub>4</sub>] and [EMIM][MeSO<sub>3</sub>] with acetone,<sup>21</sup> the binary diffusion coefficients for the IL acetone mixtures investigated in this study are about four times larger. Here, it is obvious that the distinctly larger viscosities of the pure ILs [EMIM][EtSO<sub>4</sub>] ( $\eta = 131.0$  mPa s at 293.15 K<sup>35</sup>) and [EMIM][MeSO<sub>3</sub>] ( $\eta = 205.2$  mPa s at 293.15 K<sup>36</sup>) go along with lower mutual diffusivities. Comparing the binary diffusion coefficients of the [NTf<sub>2</sub>]-based ILs with acetone, [EMIM][NTf<sub>2</sub>] shows slightly larger  $D_{12}$  values. This behavior is in accordance with the results reported by Sarraute et al.,<sup>15</sup> who found a decrease in the mutual diffusivity with increasing length of the alkyl side chain of imidazolium-based ILs infinitely diluted in water, acetonitrile, or methanol.

In contrast with the above systems, the  $D_{12}$  values for the mixtures of [EMIM][NTf<sub>2</sub>] with ethanol tend to increase from ethanol mole fractions of  $0.1$  to  $0.27$ . With further increasing  $x_{\text{et}}$ , they decrease and obviously reach a minimum between ethanol mole fractions of  $0.7$  and  $0.8$ . This could be observed for all studied temperatures and is exemplarily depicted for  $T = 283.15$  and  $323.15$  K in Figure 5. No such behavior could be found for ethanol mixtures of the IL based on the same anion, but having the cation [HMIM] with a longer alkyl chain. A possible reason for the minimum observed for the mixtures of [EMIM][NTf<sub>2</sub>] with ethanol is the existence of a critical demixing point in the respective concentration range. This speculation is supported by observations in the DLS experiments. Here, the light scattering intensities were conspicuously large in the ethanol mole fraction range from  $0.6$  to  $0.9$  for both [NTf<sub>2</sub>]-based systems. This could be caused by increasing amplitudes of the

**Table 4.** Refractive Index  $n_D$  at the Sodium Line ( $\lambda_D = 589.3$  nm), Refractive Index Difference  $n_F - n_C$  for the Fraunhofer Lines F ( $\lambda_F = 486.1$  nm) and C ( $\lambda_C = 656.3$  nm), Binary Diffusion Coefficient  $D_{12}$ , and Estimated Relative Expanded Uncertainty ( $k = 2$ ) in  $D_{12}$  for Binary Mixtures of [EMIM][N(CN)<sub>2</sub>] + Acetone

solvent	$x_{\text{solvent}}$	$T$ (K)	$n_D$	$n_F - n_C$	$D_{12}$ ( $10^{-9} \text{ m}^2 \text{ s}^{-1}$ )	$100 \times \Delta D_{12} \times D_{12}^{-1}$
acetone	0.000	283.15	1.5182	0.0132		
	0.000	293.15	1.5156	0.0135		
	0.000	303.15	1.5131	0.0133		
	0.000	313.15	1.5106	0.0132		
	0.000	323.15	1.5083	0.0130		
	0.104	283.15	1.5129	0.0134	0.125	5.9
	0.104	293.15	1.5104	0.0133	0.163	5.1
	0.104	303.15	1.5077	0.0130	0.208	8.3
	0.104	313.15	1.5054	0.0127	0.264	15.4
	0.104	323.15	1.5024	0.0129	0.279	9.1
	0.401	283.15	1.4918	0.0121	0.245	2.3
	0.401	293.15	1.4903	0.0124	0.299	3.2
	0.401	303.15	1.4875	0.0124	0.399	3.5
	0.401	313.15	1.4842	0.0121	0.471	3.4
	0.401	323.15	1.4826	0.0125	0.568	4.1
	0.702	283.15	1.4534	0.0105	0.453	1.4
	0.702	293.15	1.4520	0.0105	0.539	1.7
	0.702	303.15	1.4498	0.0104	0.616	1.7
	0.702	313.15	1.4459	0.0107	0.706	1.7
	0.702	323.15	1.4415	0.0104	0.824	2.2
	0.900	283.15	1.4057	0.0084	0.668	1.7
	0.900	293.15	1.4026	0.0085	0.760	1.7
	0.900	303.15	1.3974	0.0084	0.844	1.6

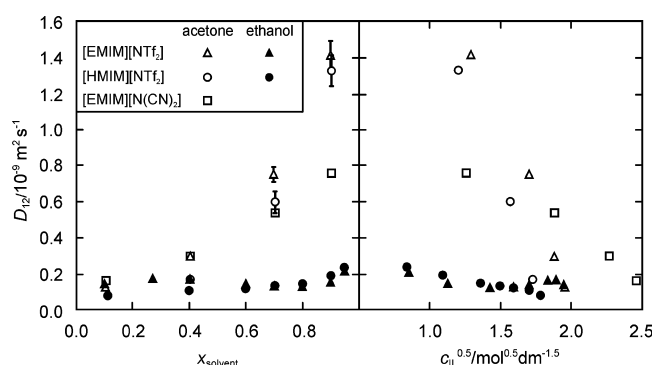


**Figure 4.** Mutual diffusivities of binary mixtures of [EMIM][NTf<sub>2</sub>], [HMIM][NTf<sub>2</sub>], and [EMIM][N(CN)<sub>2</sub>] with ethanol and acetone as a function of the solvent mole fraction and the square root of the molar concentration of the ILs at  $T = 293.15$  K.

concentration fluctuations when a critical demixing point is approached. However, the characteristic minimum for the [EMIM][NTf<sub>2</sub>] ethanol mixtures can be caused by other effects as well. For example, aqueous solutions of inorganic salts show very different  $D_{12}$  dependencies on concentration, which cannot be explained explicitly so far.<sup>37</sup> Such behaviors could also apply for the systems studied here, in which salts are dissolved in molecular solvents and, for example, might form clusters or micelles.

All systems studied here show increasing  $D_{12}$  values with increasing temperature. In Figure 6, the temperature dependence of the mutual diffusivities of the investigated systems is exemplarily illustrated for mixtures of [EMIM][NTf<sub>2</sub>] with acetone. For this, the logarithmic mutual diffusivity data are given as a

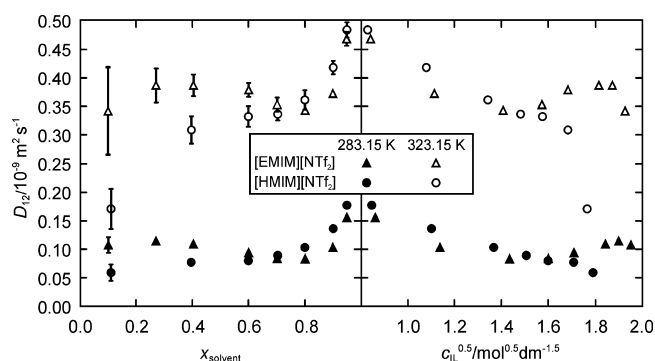


**Figure 5.** Mutual diffusivities of binary mixtures of [EMIM][NTf<sub>2</sub>] and [HMIM][NTf<sub>2</sub>] with ethanol as a function of the solvent mole fraction and the square root of the molar concentration of the ILs at different temperatures.

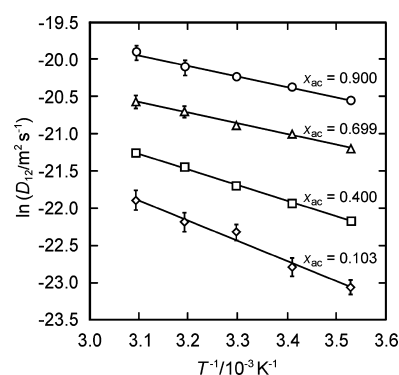


**Figure 6.** Logarithmic mutual diffusivities of binary mixtures of [EMIM][NTf<sub>2</sub>] with different mole fractions of acetone as a function of the reciprocal temperature.

function of the reciprocal temperature. In the limited temperature range probed here, the experimental data are well represented by linear fits, indicating Arrhenius-like behavior. This result is in agreement with those for the other mixtures studied here as well as with the findings reported for various IL solvent systems in the literature.<sup>15,21</sup>

## 4. CONCLUSIONS

With carefully selected experimental parameters such as the applied laser power and measurement period, accurate mutual diffusivity data for IL solvent mixtures can be obtained by the DLS technique. On this basis, a considerable influence of various anions, cations, and molecular solvents on the mutual diffusivity could be revealed. The viscosity of the pure ILs proved not to be a reliable indicator for the behavior of the binary diffusion coefficients because different types of interactions obviously dominate the respective properties. For mixtures with the protic solvent ethanol, hydrogen bonds seem to retard the diffusion process.

## AUTHOR INFORMATION

### Corresponding Author

\*Phone: +49-9131-85-29771. Fax: +49-9131-85-29901. E-mail: mr@litt.uni-erlangen.de.

### Present Address

<sup>§</sup>Institute of Chemical Reaction Engineering (CRT), University of Erlangen-Nuremberg, Egerlandstraße 3, D-91058 Erlangen, Germany

## Notes

The authors declare no competing financial interest.

## ■ ACKNOWLEDGMENTS

This work was supported by the German Research Foundation (Deutsche Forschungsgemeinschaft, DFG) by funding the Erlangen Graduate School in Advanced Optical Technologies (SAOT) within the German Excellence Initiative and via the DFG-SPP1191 priority program, Grant FR 1709/9-1. We are grateful to Matthias Bahlmann, Daniel Assenbaum, Peter Schulz, and Peter Wasserscheid from the Institute of Chemical Reaction Engineering (CRT) of the University of Erlangen-Nuremberg for the preparation of the IL [EMIM][NTf<sub>2</sub>] as well as for the water content and <sup>1</sup>H NMR analyses.

## ■ REFERENCES

- (1) Balducci, A.; Soavi, F.; Mastragostino, M. The Use of Ionic Liquids as Solvent-Free Green Electrolytes for Hybrid Supercapacitors. *Appl. Phys. A: Mater. Sci. Process.* **2006**, *82*, 627–632.
- (2) Welton, T. Room-Temperature Ionic Liquids: Solvents for Synthesis and Catalysis. *Chem. Rev.* **1999**, *99*, 2071–2083.
- (3) Schöfer, S. H.; Kaftzik, N.; Wasserscheid, P.; Kragl, U. Enzyme Catalysis in Ionic Liquids: Lipase Catalysed Kinetic Resolution of 1-Phenylethanol with Improved Enantioselectivity. *Chem. Commun.* **2001**, *2001*, 425–426.
- (4) Farag, H. K.; Endres, F. Studies on the Synthesis of Nano-Alumina in Air and Water Stable Ionic Liquids. *J. Mater. Chem.* **2008**, *18*, 442–449.
- (5) Wei, D.; Ivaska, A. Applications of Ionic Liquids in Electrochemical Sensors. *Anal. Chim. Acta* **2008**, *607*, 126–135.
- (6) Holbrey, J. D.; Seddon, K. R. Ionic Liquids. *Clean Products Processes* **1999**, *1*, 223–236.
- (7) Scovazzo, P.; Kieft, J.; Finan, D. A.; Koval, C.; DuBois, D.; Noble, R. Gas Separations Using Non-Hexafluorophosphate [PF<sub>6</sub>]-Anion Supported Ionic Liquid Membranes. *J. Membr. Sci.* **2004**, *238*, 57–63.
- (8) Haumann, M.; Dentler, K.; Joni, J.; Rüsager, A.; Wasserscheid, P. Continuous Gas-Phase Hydroformylation of 1-Butene Using Supported Ionic Liquid Phase (SILP) Catalysts. *Adv. Synth. Catal.* **2007**, *349*, 425–431.
- (9) Chauvin, Y.; Mußmann, L.; Olivier, H. Flüssige 1,3-Dialkylimidazoliumsalze als Lösungsmittel für die Katalyse in Zweiphasensystemen: durch Rhodiumkomplexe katalysierte Hydrierung, Isomerisierung und Hydroformylierung von Alkenen. *Angew. Chem.* **1995**, *107*, 2941–2943.
- (10) Steines, S.; Wasserscheid, P.; Driessen-Hölscher, B. An Ionic Liquid as Catalyst Medium for Stereoselective Hydrogenations of Sorbic Acid with Ruthenium Complexes. *J. Prakt. Chem.* **2000**, *342*, 348–354.
- (11) Richter, J.; Leuchter, A.; Palmer, G. Translational Diffusion. In *Ionic Liquids in Synthesis*; Wasserscheid, P., Welton, T., Eds.; Wiley-VCH: Weinheim, 2003; pp 162–167.
- (12) *Ionic Liquids Database (IL Thermo)*, NIST Standard Reference Database #147, <http://ilthermo.boulder.nist.gov>
- (13) Su, W. C.; Chou, C. H.; Wong, D. S. H.; Li, M. H. Diffusion Coefficients and Conductivities of Alkylimidazolium Tetrafluoroborates and Hexafluorophosphates. *Fluid Phase Equilib.* **2007**, *252*, 74–78.
- (14) Wong, C.-L.; Soriano, A. N.; Li, M.-H. Diffusion Coefficients and Molar Conductivities in Aqueous Solutions of 1-Ethyl-3-methylimidazolium-Based Ionic Liquids. *Fluid Phase Equilib.* **2008**, *271*, 43–52.
- (15) Sarraute, S.; Costa Gomes, M. F.; Padua, A. A. H. Diffusion Coefficients of 1-Alkyl-3-methylimidazolium Ionic Liquids in Water, Methanol, and Acetonitrile at Infinite Dilution. *J. Chem. Eng. Data* **2009**, *54*, 2389–2394.
- (16) Richter, J.; Leuchter, A.; Großer, N. Digital Image Holography for Diffusion Measurements in Molten Salts and Ionic Liquids—Method and First Results. *J. Mol. Liq.* **2003**, *103–104*, 359–370.
- (17) Shiflett, M. B.; Yokozeke, A. Solubilities and Diffusivities of Carbon Dioxide in Ionic Liquids: [bmim][PF<sub>6</sub>] and [bmim][BF<sub>4</sub>]. *Ind. Eng. Chem. Res.* **2005**, *44*, 4453–4464.
- (18) Morgan, D.; Ferguson, L.; Scovazzo, P. Diffusivities of Gases in Room-Temperature Ionic Liquids: Data and Correlations Obtained Using a Lag-Time Technique. *Ind. Eng. Chem. Res.* **2005**, *44*, 4815–4823.
- (19) Camper, D.; Becker, C.; Koval, C.; Noble, R. Diffusion and Solubility Measurements in Room Temperature Ionic Liquids. *Ind. Eng. Chem. Res.* **2005**, *45*, 445–450.
- (20) Shokouhi, M.; Adibi, M.; Jalili, A. H.; Hosseini-Jenab, M.; Mehdizadeh, A. Solubility and Diffusion of H<sub>2</sub>S and CO<sub>2</sub> in the Ionic Liquid 1-(2-Hydroxyethyl)-3-methylimidazolium Tetrafluoroborate. *J. Chem. Eng. Data* **2009**, *55*, 1663–1668.
- (21) Rausch, M. H.; Lehmann, J.; Leipertz, A.; Fröba, A. P. Mutual Diffusion in Binary Mixtures of Ionic Liquids and Molecular Liquids by Dynamic Light Scattering (DLS). *Phys. Chem. Chem. Phys.* **2011**, *13*, 9525–9533.
- (22) Maier, F.; Gottfried, J. M.; Rossa, J.; Gerhard, D.; Schulz, P. S.; Schwieger, W.; Wasserscheid, P.; Steinrück, H.-P. Surface Enrichment and Depletion Effects of Ions Dissolved in an Ionic Liquid: An X-ray Photoelectron Spectroscopy Study. *Angew. Chem., Int. Ed.* **2006**, *45*, 7778–7780.
- (23) Leipertz, A.; Fröba, A. P. Diffusion Measurements in Fluids by Dynamic Light Scattering. In *Diffusion in Condensed Matter*; Heitjans, P., Kärger, J., Eds.; Springer Verlag: Berlin, 2005; pp 581–620.
- (24) Fröba, A. P.; Will, S.; Leipertz, A. Diffusion Modes of an Equimolar Methane–Ethane Mixture from Dynamic Light Scattering. *Int. J. Thermophys.* **2000**, *21*, 603–620.
- (25) Shaumeyer, J. N.; Gammon, R. W.; Sengers, J. V. Photon-Correlation Spectroscopy. In *Measurement of the Transport Properties of Fluids*; Wakeham, W. A., Nagashima, A., Sengers, J. V., Eds.; Blackwell Scientific: Oxford, 1991; pp 197–213.
- (26) Berne, B. J.; Pecora, R. *Dynamic Light Scattering with Applications to Chemistry, Biology, and Physics*; Robert E. Krieger: Malabar, 1990.
- (27) Baltazar, Q. Q.; Chandawalla, J.; Sawyer, K.; Anderson, J. L. Interfacial and Micellar Properties of Imidazolium-Based Monocationic and Dicationic Ionic Liquids. *Colloids Surf., A* **2007**, *302*, 150–156.
- (28) Geng, F.; Liu, J.; Zheng, L.; Yu, L.; Li, Z.; Li, G.; Tung, C. Micelle Formation of Long-Chain Imidazolium Ionic Liquids in Aqueous Solution Measured by Isothermal Titration Microcalorimetry. *J. Chem. Eng. Data* **2009**, *55*, 147–151.
- (29) Blesic, M.; Marques, M. H.; Plechkova, N. V.; Seddon, K. R.; Rebelo, L. P. N.; Lopes, A. Self-Aggregation of Ionic Liquids: Micelle Formation in Aqueous Solution. *Green Chem.* **2007**, *9*, 481–490.
- (30) Miskolczy, Z.; Sebok-Nagy, K.; Biczók, L.; Göktürk, S. Aggregation and Micelle Formation of Ionic Liquids in Aqueous Solution. *Chem. Phys. Lett.* **2004**, *400*, 296–300.
- (31) Kinart, C. M.; Kinart, W. J.; Cwiklinska, A. Density and Viscosity at Various Temperatures for 2-Methoxyethanol + Acetone Mixtures. *J. Chem. Eng. Data* **2001**, *47*, 76–78.
- (32) González, B.; Domínguez, Á.; Tojo, J. Viscosity, Density, and Speed of Sound of Methylcyclopentane with Primary and Secondary Alcohols at T = (293.15, 298.15, and 303.15) K. *J. Chem. Thermodyn.* **2006**, *38*, 1172–1185.
- (33) Fröba, A. P.; Kremer, H.; Leipertz, A. Density, Refractive Index, Interfacial Tension, and Viscosity of Ionic Liquids [EMIM][EtSO<sub>4</sub>], [EMIM][NTf<sub>2</sub>], [EMIM][N(CN)<sub>2</sub>], and [OMA][NTf<sub>2</sub>] in Dependence on Temperature at Atmospheric Pressure. *J. Phys. Chem. B* **2008**, *112*, 12420–12430.
- (34) Widegren, J. A.; Magee, J. W. Density, Viscosity, Speed of Sound, and Electrolytic Conductivity for the Ionic Liquid 1-Hexyl-3-methylimidazolium Bis(trifluoromethylsulfonyl)imide and Its Mixtures with Water. *J. Chem. Eng. Data* **2007**, *52*, 2331–2338.



(35) Fröba, A. P.; Wasserscheid, P.; Gerhard, D.; Kremer, H.; Leipertz, A. Revealing the Influence of the Strength of Coulomb Interactions on the Viscosity and Interfacial Tension of Ionic Liquid Cosolvent Mixtures. *J. Phys. Chem. B* **2007**, *111*, 12817–12822.

(36) Hasse, B.; Lehmann, J.; Assenbaum, D.; Wasserscheid, P.; Leipertz, A.; Fröba, A. P. Viscosity, Interfacial Tension, Density, and Refractive Index of Ionic Liquids [EMIM][MeSO<sub>3</sub>], [EMIM]-[MeOHPO<sub>2</sub>], [EMIM][OcSO<sub>4</sub>], and [BBIM][NTf<sub>2</sub>] in Dependence on Temperature at Atmospheric Pressure. *J. Chem. Eng. Data* **2009**, *54*, 2576–2583.

(37) Tyrrell, H. J. V.; Harris, K. R. *Diffusion in Liquids*, 1st ed.; Butterworths: London, 1984.